1ST EUROPEAN MOBILE AIR CONDITIONING WORKSHOP
Centro Ricerche Fiat, Turin, Italy, November 29-30, 2005

05A9020

Improving energy performance in vehicle air conditioning: analysis of a liquid desiccant membrane dehumidification cycle integrated with a CO_2 refrigeration pump.

C. Isetti – University of Genoa – Italy
E. Nannei – University of Genoa – Italy
F. Vestrelli – University of Genoa – Italy

ABSTRACT

The paper reports the theoretical analysis of a hybrid air-conditioning cycle which integrates an H_2O-LiCl dehumidification cycle with a CO_2 refrigeration cycle.
The process air is cooled and dehumidified in a membrane contactor by the salt solution in order to condition the air inside the vehicle. The cooling load is handled by a CO_2 refrigeration cycle.
The diluted solution is regenerated in a second membrane contactor using heat given off by the condenser or warm water from the engine.
The power required to maintain indoor comfort conditions in summer by means of this combined cycle is compared with that required by the CO_2 cycle which directly cools the process air.
Theoretical analysis carried out by means of a Simulink code shows considerable power saving under high latent load and/or high outdoor humidity.

INTRODUCTION

Mobile air conditioning is one of the fields in which significant efforts are being made to reduce power consumption and its impact on the environment. The Montreal and Kyoto protocols have established common pathways for technological evolution and car makers and suppliers are working to build air-conditioning (AC) systems that use less power and employ refrigerants that have a lower environmental impact (GWP, LCCP) [1].

In this context, it is fundamental, more than ever, to reduce the power consumption of mobile air-conditioning systems. The traditional vapour compression equipment (V-C) tackles both sensible and latent loads by chilling the process air to below its dew-point, so that air dehumidification is intrinsically coupled with cooling [2,3]. As this operation requires the IC engine to supply a large amount of mechanical energy to the compressor, the impact on fuel consumption is considerable, particularly in hot and humid climates.

In AC, solid or liquid desiccants - such as LiCl and $CaCl_2$ solutions - enable latent loads to be handled independently from sensible loads, i.e. the humidity of the process air can be controlled independently from the temperature [2,3]. In applications in which significant latent loads are involved and when waste thermal energy is available to regenerate the desiccant, considerable power savings are possible in comparison with traditional cooling dehumidification [3,4]. Liquid desiccant processes can also improve air quality by co-absorbing pollutants into the solution [5].

Furthermore, the use of “hybrid systems” [6,7,8], i.e. direct-contact liquid desiccant cycles integrated with vapour-compression (V-C) cycles, can achieve energy benefits in

comparison with traditional V-C cycles. In these hybrid systems, the V-C cycles can operate at higher evaporation temperatures than in traditional systems, thereby saving energy mainly as a result of their higher performance coefficient (COP) [6].

Up to now, liquid desiccants have been used only for industrial AC purposes and dehumidification [2,3,4] in direct-contact plants that are not suited to mobile equipment. By adopting membrane contactors, as recently proposed [9,10,11,12], it is also possible to build compact liquid desiccant equipment for mobile AC applications. Hence, innovative hybrid membrane AC systems (H-M) that integrate V-C cycles with liquid desiccant dehumidification cycles can be envisaged. A previous study [12] involving an inverse endoreversible Carnot cycle showed that energy savings can be achieved by such an H-M system, in conditions of high latent load and/or high outdoor humidity.

The loss in simplicity of an H-M system in comparison with the traditional V-C one can be justified by its energy savings and also by the following advantages:

- using a liquid desiccant as a secondary fluid to treat the process air to the cabin allows a freer choice of refrigerants (alternative to H134a), such as the flammable H152a or propane;
- using the heat given off by the V-C condenser to regenerate the desiccant enables more compact V-C equipment, with short tubes and connections and therefore little refrigerant leakage, to be implemented close to the engine.

The aim of this study was to analyse an H-M system for mobile AC and to compare its energy performances with those of a traditional AC system. One of the most frequently considered alternative refrigerants (carbon dioxide) was used to simulate the refrigeration cycles of both systems.

TRADITIONAL AC SYSTEMS AND THE HYBRID MEMBRANE AC SYSTEM

The reference AC system consists of a refrigeration cycle using carbon dioxide as its refrigerant. Fig. 1a and 1b show the reference traditional AC system, as it is usually installed in cars, while fig. 2a and 2b show the proposed H-M system and fig. 2c a possible configuration of the components under the hood.

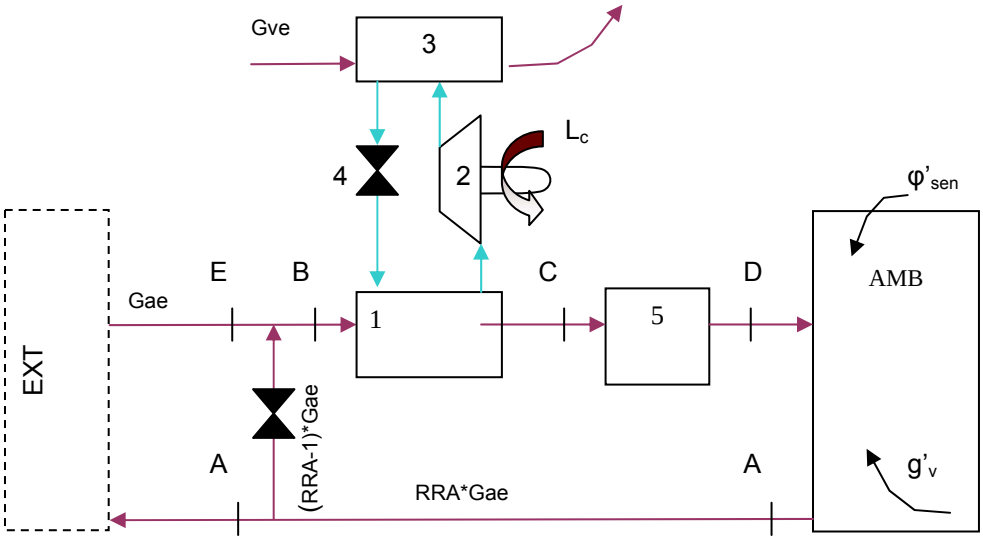

Fig. 1a Scheme of the reference AC system

AMB - vehicle cabin; EXT - outdoor environment; 1 – evaporator; 2 – compressor; 3 – condenser; 4 - expansion valve; 5 – heater; A - indoor air state; E - outdoor air state; B - mixed air state; C - air state at the outlet of 1; D - air state at the inlet of AMB.

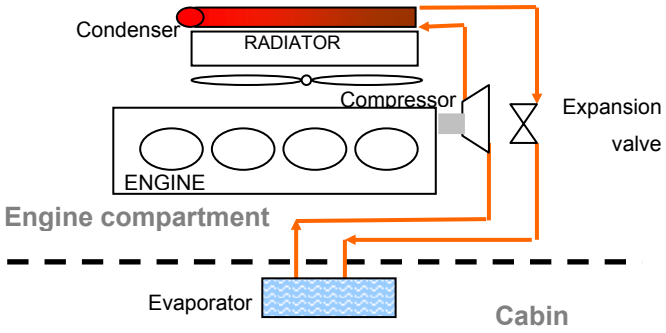

Fig. 1b Layout of the reference AC system

In traditional mobile air conditioning, the air to be treated by the system (fig. 1a) - totally renewed or fully recycled - is conveyed to the heat exchanger (1) (evaporator) and then heated by means of the cabin heater (2) in order to obtain comfortable conditions in the AMB. The thermodynamic process is shown in fig. 1c.

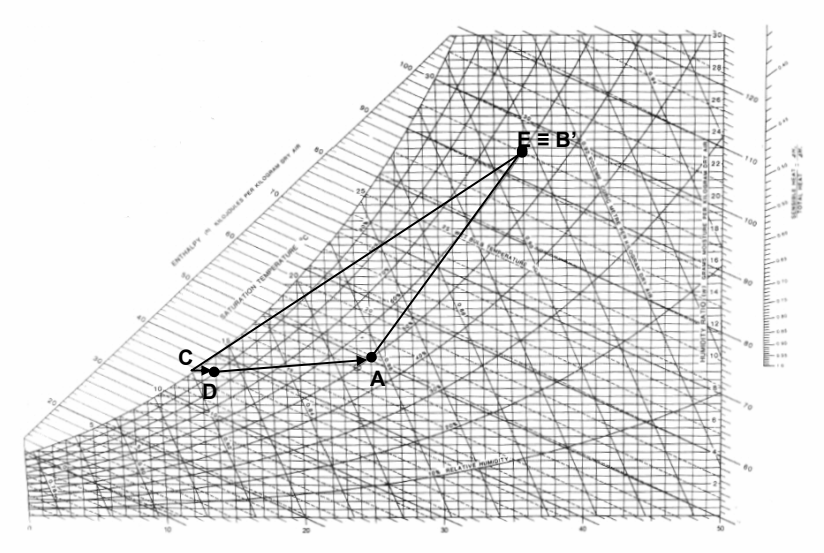

Fig. 1c Reference AC cycle

The same air-side layout has also been considered for the H-M system, in which the air passes through the membrane contactor (6), where it is cooled down and dehumidified by means of simultaneous heat and mass transfer processes, before being conveyed to the AMB. The thermodynamic process is shown in the Carrier diagram in fig. 2d.

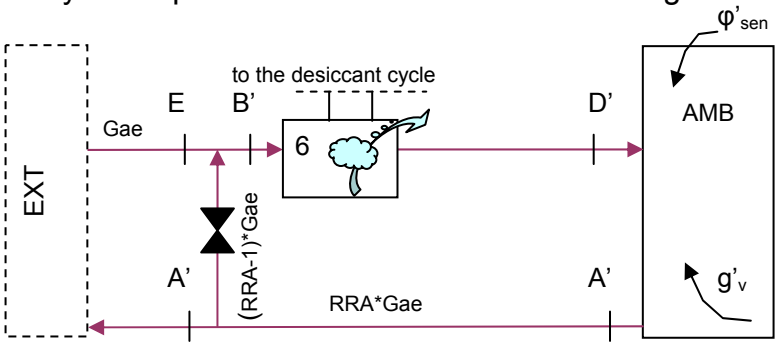

Fig. 2a Scheme of the hybrid membrane AC system

AMB - vehicle cabin; EXT - outdoor environment; 6 – dehumidifier contactor; A' - indoor air state; E - outdoor air state; B' - mixed air state; D' - air state at the inlet of AMB.

In the solution-side loop, depicted in fig. 2b, there are two membrane contactors (1,

7): one to dehumidify the air (1) and the other to regenerate the diluted solution (7). The solution in the dehumidification loop must be maintained at a constant concentration and cooled in order to condition the air, while the heated solution in the contactor regenerator is re-concentrated. The cooling unit is therefore used as a heat pump to transfer heat from the dehumidification loop to the regeneration loop.

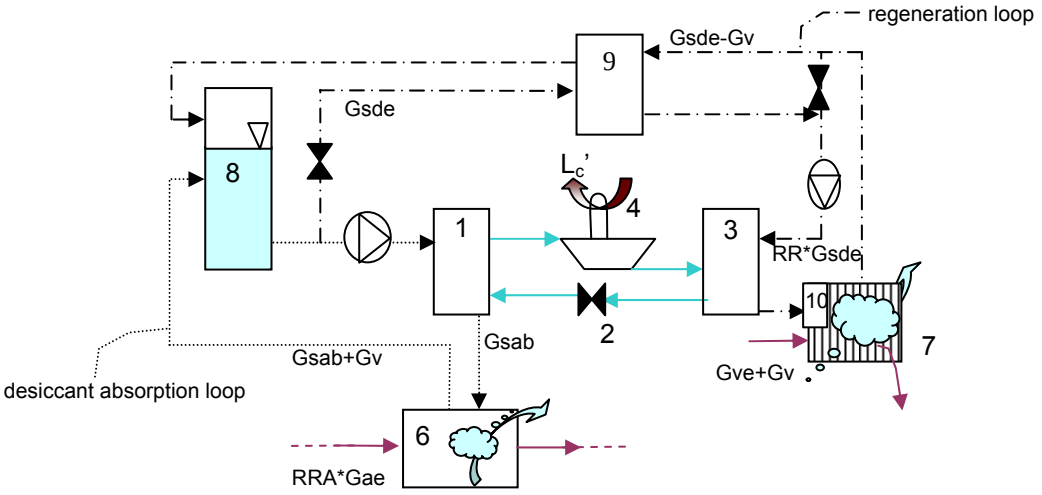

1 – evaporator; 2 – compressor; 3 – condenser; 4 - expansion valve; 7 – regeneration contactor; 8 – solution tank; 9 – recuperator heat exchanger; 10 – solution heater.

Fig. 2b Particular of the desiccant cycle

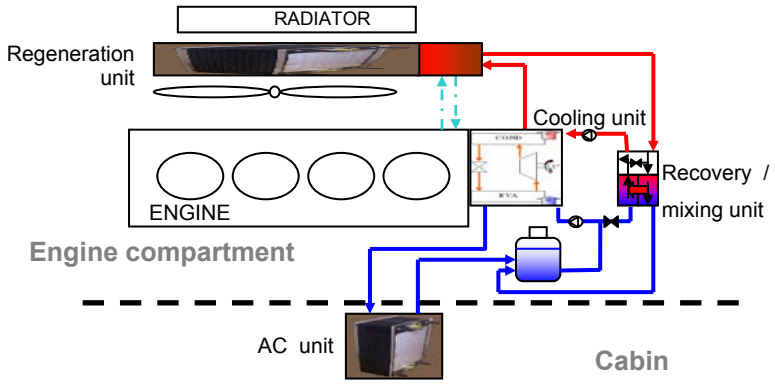

Fig. 2c Layout of the hybrid membrane AC system

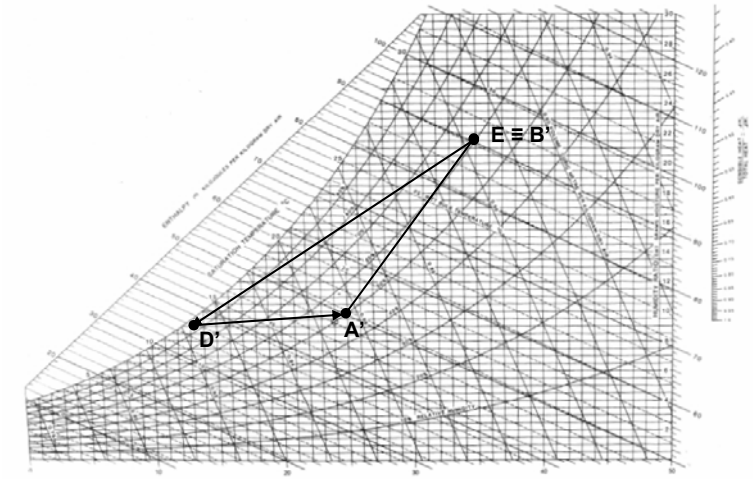

Fig. 2d Hybrid membrane AC cycle

As the desiccant solution becomes diluted during the absorption process, it must be re-concentrated in the regeneration loop, in order to keep the concentration constant. The scheme of the heat and mass transfer loop (desiccant cycle) is detailed in fig. 2b. The diluted solution, coming from (6), flows into the tank (8), where the concentration is restored to the required value. This process takes place in the regeneration loop and is carried out by first preheating the solution in the recovery heat exchanger (9) and subsequently increasing the solution temperature by means of the waste heat from the condenser refrigeration cycle (3). The solution then flows into the regenerator contactor (7), where the vapour is discharged outside into the outdoor air (E) stream thereby increasing the solution concentration. The warm concentrated solution returns to the tank through the recovery heat exchanger (9), in counter-current with the cold solution coming from (8). In the absorption loop, the solution is cooled down by the evaporator of the V-C cycle (1).

At the highest latent loads, the waste heat from the engine is used to heat the solution in the heat exchanger (10).

In the H-M cycle, a regeneration ratio has been introduced; this is defined as:

$$RR = \frac{Gs_{de} + Gs_{derec}}{Gs_{de}} \qquad (1)$$

where Gs_{de} is the flow rate to the regeneration loop, and Gs_{derec} is the flow rate recycled in the loop. Furthermore, the ratio between Gs_{de} and the solution flow rate through the absorber Gs_{ab} is defined as follows:

$$Gs_{ratio} = \frac{Gs_{de}}{Gs_{ab}}. \quad (2)$$

The solution temperatures and concentrations which establish in the two loops control the heat and vapour transfer in the dehumidifier and in the regeneration contactor. In steady state conditions the absorbed water vapour rate in the contactor (6) is equal to the desorbed water vapour rate in the other contactor (7).

Simulation input and analysis

The computer simulations of the two CO_2 refrigeration AC systems (reference and HM systems) were carried out assuming for both systems:

- totally renewed air (RRA=1);
- the same temperature and relative humidity of the outdoor air;
- negligible blower power consumption to move air to cabin;
- negligible mechanical power required for the desiccant flow in the absorption and desorption loops;
- ambient volume V = 3 m^3;

Both systems handle the same outdoor air flow rate Ga_e (E state) and re-circulated air flow rate Ga_{rec} so that the total air flow rate into the AMB ($Ga = Ga_e + Ga_{rec}$) is the same. The air flow Ga into the AMB handles the indoor sensible and latent heat loads to match indoor conditions (states A and A' respectively) allowing the same human comfort indexes PMV and PPD. In both systems the air re-circulation ratio RRA is defined as:

$$RRA = \frac{Ga_e + Ga_{rec}}{Ga_e} \qquad (3)$$

In modelling the CO_2 cycle, the CO_2 thermodynamic properties were derived from [13] and the characteristics of the Lynd compressor for automotive application were taken from its efficiency chart [14].

The performances of the membrane contactors refer to a module provided by the GVS Company and depicted in fig.3. In the simulation, the dimensions of the contactor core were set at 400x340x210mm, corresponding to two modules in series on the air path.

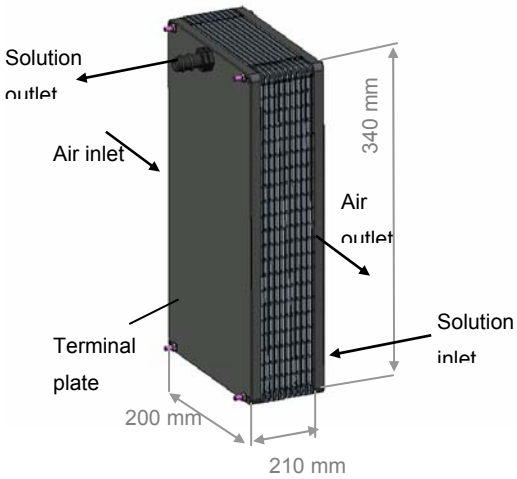

Fig. 3 Thermal welded cross-flow membrane contactor

The membrane was composed of a PTEF layer (≈ 70 μm) with nominal porosity 0.2 μm laminated on a polyester supporting layer of up to 170 μm total thickness; its permeability δ was in the range $4.65*10^{-11} \div 7.35*10^{-11}$ (kg/(m^2 s Pa) (i.e. $0.95 < R_{et} < 1.5$ (m^{2}Pa/W)) as tested at DIPTEM [15].

A description of the equations used to evaluate vapour flux through the membrane and a description of the theoretical and experimental results obtained at DITEM on thermal welded contactors is given in [10,15]. Fig. 4 shows the vapour fluxes absorbed by the salt solution as a function of the air flow Ga. The continuous line shows the predicted values obtained with the two different membrane permeabilities mentioned above.

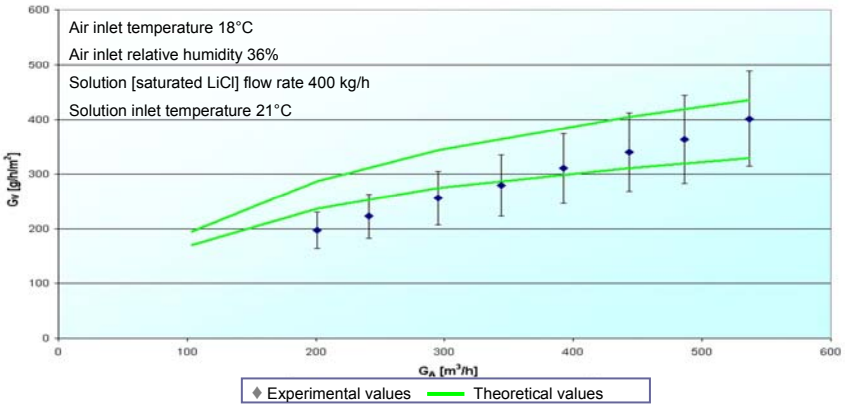

Fig. 4 -Vapour fluxes as a function of air flow rate: experimental and computed results [15]

The performances of the two systems were compared by means of a SIMULINK code (MATLAB environment) that provides a graphical user interface for building a multi-component system as a succession of blocks. Each block represents a system component

(for instance, the absorber and the desorber contactor, the economiser heat exchanger and so on) in which the inlet and the outlet variables are linked together by means of the governing equations describing the behaviour of the component itself.

The thermodynamic properties of moist air were modelled according to [2], while the properties of the LiCl solution were modelled on the basis of experimental data reported in literature [16÷19]. For both systems, the calculations were made in order to obtain the same conditions of human comfort in the AMB, i.e. the same predicted mean vote (PMV) and predicted percentage of dissatisfied (PPD) cloth thermal resistance I_{cl}, mean radiant temperature t_{mr}, air velocity v and metabolic rate M/A_b [20,21], as reported in Table 1.

Table 1

I_{cl} [clo]	t_{mr} [°C]	v [m/s]	M/A_b [W/m^2]	PMV [-]	PPD [-]
0.5	28	0.2	72	0.24	6.2

The same PMV can be achieved with an air temperature $t_{A^*} > 25$ and $\phi_{A^*} < 50\%$ or with $t_{A^*} < 25$ and $\phi_{A^*} > 50\%$, so that the increased dehumidification in the first case will be accompanied by a greater latent load.
All simulations were carried out assuming the input data specified in tables 2, 3 and 4.

Table 2: outside and indoor air, sensible and latent load, air flow rate and RRA parameter

t_E [°C]	ϕ_E [%]	t_A [°C]	ϕ_A [%]	φ'_{sen} [W/m^3]	g_v' [g/(hm^3)]	G_{vE} [m^3/h]	Ga [kg/h]	RRA [-]	Ga_e [kg/h]
35	60	25	50	450	115	1000	400	1	400

Table 3: AC standard cycle, characteristics of the heat exchangers

Heat exchanger (1)	U_1= 150 [W/m^2 K]; A_1= 1.1 [m^2]
Heat exchanger (3)	U_3= 150 [W/m^2 K]; A_3/A_1=0.91; A_3 = 1.0 [m^2]

Table 4: H-M cycle

Heat exchanger (1)	U_1^*= 2000 [W/m^2 K]; A_1^*= 1.5 [m^2]
Heat exchanger (3)	U_3^*= 1500 [W/m^2 K]; A_3^*/A_1^*=0.64; A_3^*= 0.96 [m^2]
Regenerator (9)	U_9^*= 400 [W/m^2 K] A_9^*= 0.5 [m^2]
Gs ratio	0.1 [-]
RR	10 [-]
At the inlet (1)	Gs_{ab} = 900 [kg/h]
At the inlet (3)	RR Gs_{de} = 900 [kg/h]
From (8) to (9)	$Gs_{de} = Gs_{ab} \cdot Gs_{ratio}$ = 90 [kg/h]
Membrane contactor (6)	A_6^* = 7 [m^2]; $\delta \approx 3.5-7-14\cdot10^{-11}$ $[kg/(msPa)]$
Membrane contactor (7)	A_7^*/A_6^* = 1.18; A_7^* = 8.3 [m^2]; $\delta \approx 14\cdot10^{-11}$ [kg/(msPa)]

The values of thermal transmittances for all heat exchangers, in both traditional and hybrid systems, were assumed in accordance with heat exchanger practice [22].

The energy performances of the two cycles were compared in steady state conditions by adjusting the heat flux at the evaporator (1) of the of the H-M cycle and marching in time until the same comfort parameters (PMV and PPD) were reached in the AMB for t_E = 35 and Φ_E = 60 %.

RESULTS

The mechanical power required by the two cycles in order to achieve the same comfort conditions in the AMB were first computed on the basis of the data in Tables 1, 2, 3 and 4, in order to evaluate the influence of the relative humidity of the outside air. Fig. 5 shows the trend in the percentage mechanical power saving (MPS) on adopting three different membrane permeabilities for the dehumidifier.

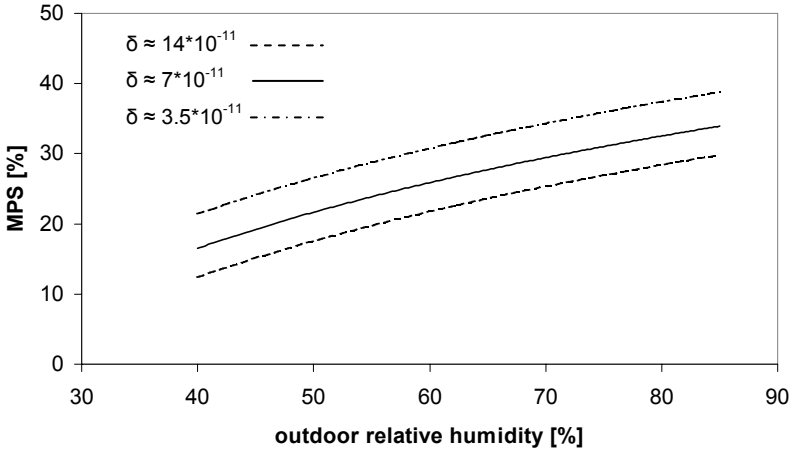

Fig. 5 MPS for different external relative humidity values and different membrane permeabilties of the dehumidifier

The proposed H-M system is seen to achieve considerable power savings at the highest values of outdoor relative humidity; furthermore the saving increases when the membrane permeability decreases.

In addition, a higher efficiency of the recovery heat exchanger from 0.54 to 0.71 yields a higher MPS, as shown by the theoretical results obtained for a membrane permeability $\delta = 7 \cdot 10^{-11}$ (kg/m^2 s Pa) and depicted in Fig 6. This effect is mainly due to the more efficient thermal separation of the absorption and regeneration cycles: indeed, the lower the heat flow rate transferred from the regeneration loop to the absorption loop, the less the heat flow to be handled by the evaporator, and therefore the lower the power consumption of the cooling unit.

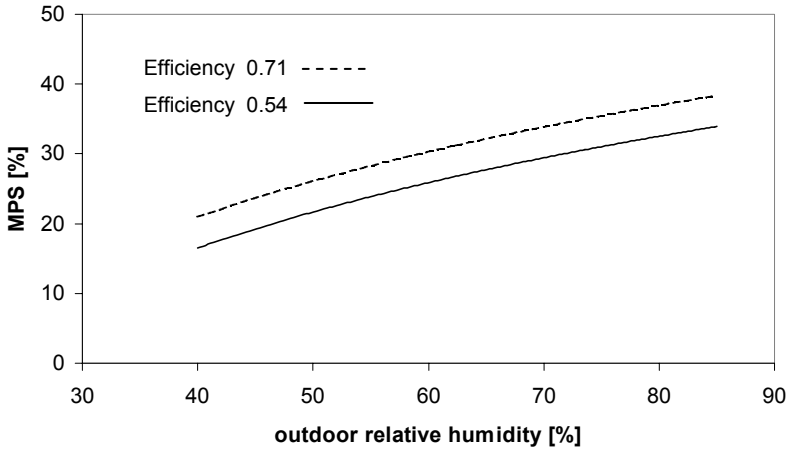

Fig. 6 MPS for different values of outside relative humidity and recovery heat exchanger efficiency

Finally, further calculations were made with the same input data (Tables 1, 2, 3, 4) – except of ϕ_E set equal to 50% - to assess the influence of indoor vapour production g_v'. Considering that the base value of 115 g/h·m^3 corresponds to a vapour production of driver plus four passengers, other cases with more or less passengers have been simulated.

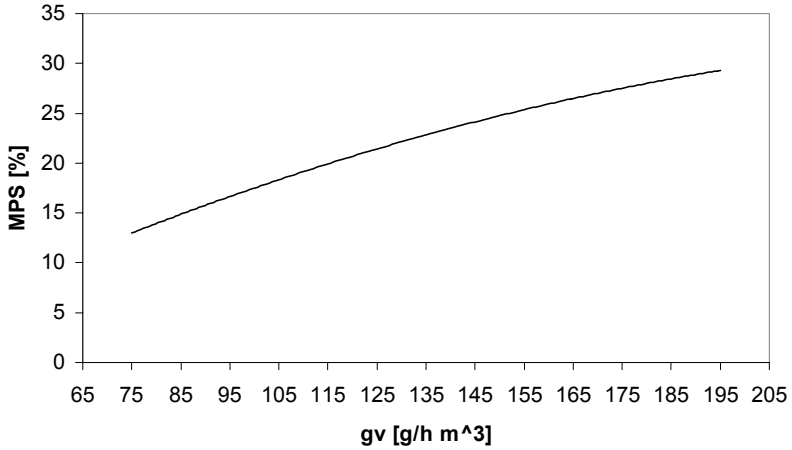

Fig. 8 MPS for different indoor vapour production values

Results depicted in fig. 8 show that MPS increases with the indoor vapour production; a power saving of about 30% can be obtained when the vapour production rises to 190 g/h m^3.

CONCLUSIONS

The following conclusions can be drawn:

- in summer, the H-M cycle achieves comfortable indoor conditions, with power saving of up to about 35 % in comparison with a traditional CO_2 refrigeration cycle;
- power saving increases as the relative humidity of the outdoor air and the latent loads in the controlled ambient increase; the higher energy saving is not achieved by using the membrane with the highest vapour permeability in the dehumidification contactor;
- energy saving increases with the efficiency of the regenerator heat exchanger.

SYMBOLS

A	surface (m^2)
COP	coefficient of performance (-)
g'_v	internal vapour production in AMB (g/hm^3)
Ga	mass flow rate into the conditioned cabin (kg/h)
Ga_e	renewal air mass flow rate (kg/h)
Ga_{rec}	recirculated air mass flow rate (kg/h)
G_{vE}	outdoor air flow rate throughout (3) and (7) (m^3/h) of fig. 2b
G_v	absorbed/desorbed vapour mass flow rate in the H-M cycle (kg/h)
Gs_{ab}	LiCl solution mass flow rate at the inlet of the absorber (6) (kg/h)
Gs_{de}	LiCl solution mass flow rate to the desorption loop (kg/h)
Gs_{derec}	LiCl solution re-circulated mass flow rate (kg/h)
Gs_{ratio}	ratio between Gs_{de} and Gs_{ab}
I_{cl}	thermal resistance of clothing of occupants in AMB (clo)
MPS	mechanical power saving (%)
M/A_b	metabolic specific power of occupants in AMB (W/m^2)
PMV	predicted mean vote (-)
PPD	predicted percentage of dissatisfied (%)
R_{et}	membrane mass transfer resistance to latent flux ($m^2/Pa\ W$)
RRA	air re-circulation ratio (-)
RR	solution re-circulation ratio in the desorption loop (-)
t	temperature (°C)
t_{mr}	radiant mean temperature of AMB (°C)
U	overall heat transfer coefficient (W/m^2)
v	mean air velocity in AMB (m/s)
V	volume of the conditioned cabin (AMB) (m^3)

Greek Symbols

δ	membrane permeability ($kg/(m^2\ s\ Pa)$)
φ'_{sen}	sensible heat load (W/m^3)
ϕ	relative air humidity (%)

Subscripts

1,2,3,4,…,8	refer to the i_{th} component
A,B,C,D,E	refer to the i_{th} air state of the traditional AC
A*,B*,D*	refer to the i_{th} air state of the H-M cycle

REFERENCES

1. Armin Hafner, Petter Nekså and Jostein Pettersen, Life Cycle Climate Performance (LCCP) of Mobile Air-Conditioning Systems with HFC-134a, HFC-152a and R-744, *MAC-Summit 2004, Washington*
2. ASHRAE Handbook, *HVAC Systems and Equipment*, SI Edition, Atlanta, USA, 1992.
3. ASHRAE Handbook, *Fundamentals*, SI Edition, Atlanta, USA, 1993.
4. A. Lowenstein, S. Slayzak, J. Ryan and A. Pesaran, Advanced Commercial Liquid-Desiccant Technology Development study, *NREL/TP-550-24688*, 1998.
5. T. W. Chung, T. K. Ghosh, A. L. Hines, D. Novosel, Removal of Selected Pollutants from Air During Dehumidification by Lithium Chloride and Triethylene Glycol Solutions, *Proc. of the 1993 Winter Meeting of ASHRAE Transactions*, ASHRAE, Atlanta, USA, pp. 834-841, 1993.
6. J.R Howell and J.L. Peterson., Preliminary Performance Evaluation of a Hybrid Vapor Compression/Liquid Desiccant Air Conditioning System, ASME Paper 86-WA/Sol. 9, Anaheim, Calif., Dec. 1986.
7. Y.K. Yadav, Vapour-Compression and Liquid-Desiccant Hybrid Solar Space-Conditioning System for Energy Conservation, *Renewable Energy*, 6 (7), pp. 719-723, 1995.
8. J.W. Studak and J.L. Peterson, A preliminary Evaluation of Alternative Liquid Desiccants for a Hybrid Desiccant Air Conditioner, *Proc. of the Fifth Annual Symposium on Improving Building Energy Efficiency in Hot and Humid Climates*, pp. 155-159, Houston, TX, Sept. 13-14, 1988.
9. C. Isetti, E. Nannei and A. Magrini, On the Application of a Membrane Air-liquid Contactor for Air Dehumidification, *Energy and Buildings*, vol. 25, pp. 185-193, 1997.
10. S. Bergero, A. Chiari and C. Isetti, On the Performance of a Plane-plate Membrane Contactor for Air Dehumidification, *Proc. of the 7th RHEVA World Congress Clima 2000*, Napoli, 2001.
11. S. Bergero, A. Chiari and E. Nannei, Energy Saving in Air Conditioning Systems: Study of an Innovative Passive Technique Based on Membrane Contactors and Hygroscopic Solution. *IPLEA*, Toulose, 2002.
12. C. Isetti, E. Nannei, Energy saving in air conditioning: analysis of a liquid desiccant membrane dehumidification cycle integrated with an endoreversible Carnot heat pump in summer conditions. *Eurotherm Seminar 72: Thermodynamics heat and mass transfer of Refrigeration machines and heat pumps,* Valencia, 2003
13. Cavallini A.: “Heat transfer and energy efficiency of working fluids in mechanical refrigeration”, Bullettin IIR, 6/2002, pp. 5-21, 2002.
14. Suess J., Veje C., Development and performance measurements of a small compressor for transcritical CO_2 applications, Proc. Int. Compressor Eng. Conf. Purdue, 2004.
15. C. Isetti, E. Nannei and L. Marengo, Scambiatori piani a membrana nel trattamento dell’aria: risultati sperimentali e numerici. CDA, n°9, pp. 52-58, 2005.
16. B. Gazinski and E. Szczechowiak, Die thermodynamischen grundlagen der luftenfeuchtung mit hilfe der wässerigen lithiumbromid und lithiumchlorid-lösungen, *Ki Klima-Kälte*, vol. 1, pp. 509-515, 1984.
17. E. F. Johnson and C. M. Melvin, Thermodynamic Properties of Aqueous Lithium Chloride Solutions, *J. Physical Colloid Chemistry*, vol. 55, pp. 257-281, 1951.
18. T. Uemura, Studies on the Lithium Chloride-water Absorption Refrigerating Machine, *Technology reports of the Kansai University*, Osaka, Japan, vol. 9, 1967.
19. I.O. Zaytsev and G.G. Aseyev, *Properties of Aqueous Solutions of Electrolytes*, CRC Press, Boca Raton, 1992. W.M.
20. ASHRAE (1981), *Thermal environmental conditions for human occupancy ASHRAE*

STANDARD 55-1981, ASHRAE, Atlanta 1981.
21. P.O. Fanger (1982), *Thermal comfort*; R.E. Krieger Publishing Company, Malabar, 1982.
22. Rohsenow, J.P. Hartnet and E.N. Ganic, *Handbook of Heat Transfer Fundamentals*, MC Graw Hill Book, 1985.